NUMERICAL ANALYSIS OF THE BYPASS VALVE IN A LOOP HEAT PIPE

Michel Speetjens & Camilo Rindt

Laboratory for Energy Technology
Mechanical Engineering Department
Eindhoven University of Technology
The Netherlands

Mai 2007

MATEO-ANTASME deliverable 9.2

PROJECT PART-FINANCED BY THE EUROPEAN UNION

Introduction

The present study concerns a follow-up study on the integral thermodynamical analysis of the bypass valve discussed in Speetjens & Rindt (2006). This bypass valve is a crucial component in the loop heat pipe (LHP) that, in turn, is part of the cryo-cooling system for the thermal control of the Alpha Magnetic Spectrometer. The principal purpose of the bypass valve is averting freezing of the working fluid (Propylene) – and thus malfunctioning of the LHP – by termination of its circulation through the LHP in case the evaporator pressure drops below a preset minimum value. Further background and details are in Speetjens & Rindt (2006).

The integral analysis of the bypass valve in Speetjens & Rindt (2006) leans on the assumption of (i) inviscid flow, (ii) uniform inlet/outlet conditions and (iii) quasi-static conditions. The present analysis seeks to determine whether viscosity, non-uniformity and non-quasi-static effects (e.g. due to fluid inertia) are significant, which requires resolution of the fluid flow and heat transfer in the interior of the bypass valve. This analysis is performed through numerical simulation of the two steady-state operating conditions of the bypass valve by means of the finite-volume method (FVM). To this end we use the commercial package Fluent.

Operating conditions and material properties

The present analysis is, as opposed to the non-dimensional study in Speetjens & Rindt (2006), performed in dimensional quantities so as to specifically characterise the actual bypass valve. The geometry and corresponding dimensions of the bypass valve and the operating conditions are specified in Bodendiek et al. (2005):

- geometry as shown schematically in Figure $1a$ (dimensions as in Bodendiek et al. (2005));
- temperature range at the inlet: $245\,K \leq T \leq 265\,K$;
- saturation conditions at the inlet;
- negligible radiative heat loss through the walls;
- heat intake by the evaporator $\dot{Q}_e \sim \mathcal{O}(30\,W)$; full liquid-to-vapour phase change in evaporator: $\dot{Q}_e = \dot{m}h_{fl}$, with $\dot{m}$ the mass flow and h_{fl} the evaporation enthalpy of the Propylene;
- zero-gravity conditions.

The working medium of the LHP is Propylene (C_3H_6). The corresponding thermodynamical and material inlet properties are ($ALLPROPS$):

$$p_{245} = 2.3bar,\ \rho_{245} = 6.0\frac{kg}{m^3},\ h_{fl,245} = 416.4\frac{kJ}{kgK},\ c_{p,245} = 1426\frac{J}{kgK},\ \mu_{245} = 15.7\mu Pas,$$
$$p_{265} = 4.6bar,\ \rho_{265} = 9.7\frac{kg}{m^3},\ h_{fl,265} = 416.4\frac{kJ}{kgK},\ c_{p,265} = 1568\frac{J}{kgK},\ \mu_{265} = 16.3\mu Pas,$$

completed by $c_{245} = 227.5m/s$ and $c_{265} = 228.1m/s$ as propagation speeds of sound, with the subscripts referring to the inlet temperature. Note that, somewhat counter-intuitively, density and kinematic viscosity increase with temperature due to the fact that, given saturation

conditions are maintained, the pressure also increases. The above leads to the following operating conditions at the inlet:

$$\dot{m} = \frac{\dot{Q}_e}{h_{fl}} \sim \mathcal{O}(50\mu g/s), \;\; U = \frac{\dot{m}}{\rho A} \sim \mathcal{O}(3m/s), \;\; Re = \frac{Ud\rho}{\mu} \sim \mathcal{O}(3000), \;\; Ma = \frac{U}{c} \sim \mathcal{O}(0.015)$$

with $A = \pi d^2/4$ the inlet area and $d_i = 2mm$ the inlet diameter and Re and Ma the well-known Reynolds and Mach numbers, respectively.

Mathematical model for the fluid flow and heat transfer in the bypass valve

The assumptions underlying the analysis by Speetjens & Rindt (2006) admit description of the fluid flow and heat transfer in the bypass valve by the integral conservation laws for mass and energy of classical thermodynamics (Cengel & Boles (2002)). Dismissal of the assumption of quasi-static conditions requires this model be extended by the conservation law for momentum. Furthermore, allowing for viscous effects and non-uniform inlet/outlet conditions introduces viscous terms in the momentum and energy equations and implies that specific boundary conditions on both inlet and outlet as well as on stationary walls become significant and resolution of the problem within the interior of the bypass valve becomes necessary. The model that describes the present problem thus consist of the generic conservation laws for mass, momentum and energy according to Hirsch (1988) complemented by suitable boundary conditions. However, the operating conditions in the bypass valve admit simplification of this generic model.

The fluid in question (Propylene) is gaseous and, inherently, we in principle have a compressible and non-isothermal flow. However, the following considerations admit reduction to a fully incompressible and isothermal flow that can be tackled with standard numerical techniques:

1. The present Reynolds number approximately coincides with the lower end of the transition regime $2300 < Re < 10^4$. This basically implies laminar flow conditions (VDI Wärmeatlas (2002)).

2. The present Mach number is well below unity. This to good approximation implies incompressible flow and, consequently, a density that is dependent upon the temperature only: $\rho = \rho(T)$ (Schlichting & Gersten (2000)).

3. The integral thermodynamical analysis revealed that adiabatic conditions (i.e. negligible heat loss through the walls) lead to nearly iso-thermal conditions, suggesting that internal temperature variations are small (Speetjens & Rindt (2006)). This, combined with the small length scales involved with the bypass valve, admits further reduction of the simplified flow problem to the well-known Boussinesq approximation, in which density variations due to thermal effects are restricted to an additional gravitational term in the momentum equation (Kundu (1990)). However, the bypass valve operates under zero-gravity conditions, meaning said gravitational term drops out here.

The above considerations simplify the original flow to an incompressible and isothermal flow that is governed by

$$\nabla \cdot \boldsymbol{u} = 0, \qquad \rho \boldsymbol{u} \cdot \nabla \boldsymbol{u} = -\nabla p + \mu \nabla^2 \boldsymbol{u}, \qquad \rho c_p \boldsymbol{u} \cdot \nabla T = \lambda \nabla^2 T + \phi, \tag{1}$$

consisting of the standard Navier-Stokes equations and the energy equation, with ϕ representing viscous heat production.

Relations (1) constitute the model that, complemented by suitable boundary conditions, describes the fluid flow and heat transfer in the bypass valve. The flow boundary conditions are: prescribed mass flow at inlet; outflow conditions at the outlet; no-slip conditions at the interior walls. The thermal boundary conditions are: inlet conditions as specified above; outflow conditions at the outlet; adiabatic interior walls. The laminar flow conditions allow application of standard numerical techniques without the need for turbulence models.

Numerical analysis of the bypass valve

Relevant characteristics for practical purposes are total pressure drop and temperature changes as a function of inlet conditions. Further relevant property is occurrence of high-pressure zones within the interior of the bypass valve, which may serve as indicators for the risk of internal condensation. The numerical analysis is restricted to the states at minimum ($T = 245K$) and maximum ($T = 265K$) inlet temperatures for both operating modes. These states are examined for the mass-flow range $50\mu g/s \leq \dot{m} \leq 100\mu g/s$ and are considered representative of states at intermediate $245K < T < 265K$.

Figure 1*a* shows the cross-section of the bypass valve (panel *a*) and the corresponding computational meshes of the closed (panel *b*) and open (panel *c*) operating modes. (Note that for legibility a coarser mesh than that actually used is shown.) The bypass valve is symmetric about the plane spanned by the centrelines of the inlet/outlet pipes and the centreline of the bypass valve. The three-dimensional internal flow and temperature field are also assumed symmetric about this plane. This symmetry admits reduction of the computational domain to one of the two subdomains divided by this plane of symmetry. Thus shown meshes concern only one such subdomain.

Numerical simulations of both operating modes reveal that the bypass valve approaches an isothermal state for the operating ranges considered here. Deviations ΔT of the internal temperatures deviate from the prescribed inlet temperature T_i are typically $\Delta T \sim \mathcal{O}(0.002K)$. This signifies an essentially isothermal state $T(\boldsymbol{x}) = T_i$ at any position $\boldsymbol{x}$ within the bypass valve. This implies that viscous heat generation is negligible and thus consolidates the assumption of an isothermal flow.

Fluid flow and heat transfer: closed mode

Figure 2 gives the typical velocity field in the closed mode. Shown are the velocity vectors (panel *a*) and the velocity magnitude (panel *b*), with color-coding as indicated, in the symmetry plane for $\dot{m} = 70\mu g/s$ and $T = 245K$. The plots clearly reveal the fluid flowing directly from the inlet pipe via the lower-right part of the stem to the outlet. Fluid motion in other regions is negligible. The organised and confined flow structure and confinement of fluid motion to said regions signifies in essence laminar flow conditions.

Figures 3*a* and *b* give close-ups of the velocity vectors and velocity magnitude, respectively, in the region with significant fluid flow. The entering flow has a developed profile that is deflected downward by the stem towards the inlet of the outlet pipe. The fact that below the stem the velocity magnitude remains at values comparable to that in the inlet and outlet pipes, despite considerable narrowing of the throughflow area, implies spreading of the fluid

underneath the stem in lateral direction (i.e. away from shown symmetry plane) after leaving the inlet and subsequent concentration upon reaching the inlet of the outlet pipe. The perpendicular orientation of the outlet pipe relative to the incoming flow causes a sudden redirection of the fluid motion and leads to an asymmetric velocity profile within the outlet pipe. This asymmetry persists throughout the outlet pipe and thus means that its length is insufficient for the flow to fully develop.

Figures 3*c* and *d* give close-ups of the velocity vectors and velocity magnitude, respectively, in the abovementioned region for the same mass flux ($\dot{m} = 70\mu g/s$) yet at temperature $T = 265K$. The plots show that differences with the case $T = 245K$ are marginal. The flow structure is virtually identical; only its magnitude is slightly smaller. The latter is a direct consequence of the fact that $\rho_{265}/\rho_{245} > 1$, which for identical $\dot{m}$ implies $U_{265}/U_{245} < 1$. The similarity in structure with small changes in conditions is a further indication of the essentially laminar nature of the flow. This substantiates the assumption of laminar flow conditions that underly the simplified flow model and corresponding numerical methods used here.

Typical pressure fields for the closed mode equal that shown in Figure 4 for $\dot{m} = 70\mu g/s$. Top and bottom rows correspond with $T = 245$ and $T = 265$, respectively; left and right columns correspond with full views and close-ups, respectively. The full view in panel *a* clearly reveals the approximately linear pressure gradient in the inlet pipe (consistent with the developed velocity field) and the pressure build-up at the right side of the stem due to deflection of the fluid. The close-up in panel *b* exposes weaker pressure build-up regions on the valve wall directly below the high-pressure region at the stem and at the left side of the inlet of the outlet pipe. The latter results from the redirection of the flow mentioned before. Panel *b* furthermore shows that the pressure distribution within the outlet pipe is equally asymmetric as the velocity field. The latter leads to a weak pressure gradient transverse to the flow direction. Figures 4*c* and *d* show full view and close-up of the pressure field, respectively, for $T = 265$. The pressure field for $T = 265$ is, similar as for the velocity field, of essentially the same structure as that for $T = 245$, albeit with weaker magnitude. Pressure build-up regions occur at the same locations yet are less profound.

Important for the thermodynamical state of the fluid is that in the high-pressure zone at the right side of the stem the local pressure exceeds the inlet pressure. Moreover, the pressure excess at the high-pressure zone increases with increasing mass flow $\dot{m}$. This implies that, given saturation conditions at the inlet and an isothermal state (see before), locally $T = T_{sat}$ and $p > p_{sat}$ ('sat' denotes saturation) and thus a local pressure above the saturation pressure. Thus the simulations, though concerning incompressible flow, strongly suggest that condensation (or even freezing) may occur in the direct proximity of the right side of the stem due to compression of a saturated fluid (Cengel & Boles (2002)). Such phase changes must be avoid, as they are likely to obstruct throughflow by narrowing the flow passage or may even lead to full blockage, thus seriously compromising the performance of the bypass valve and, inherently, the LHP. However, the above reveals that flow structure and qualitative thermodynamical state are essentially the same for slight variations in inlet conditions. Thus condensation (or freezing) can be avoided by ensuring a slightly superheated state at the inlet. This "safety superheat" must increase with increasing $\dot{m}$.

Fluid flow and heat transfer: open mode

Figure 5 give the global velocity field in the symmetry plane for $\dot{m} = 70\mu g/s$ and $T = 265K$ for open-mode conditions. Here the fluid must, contrary to the closed mode, flow fully around

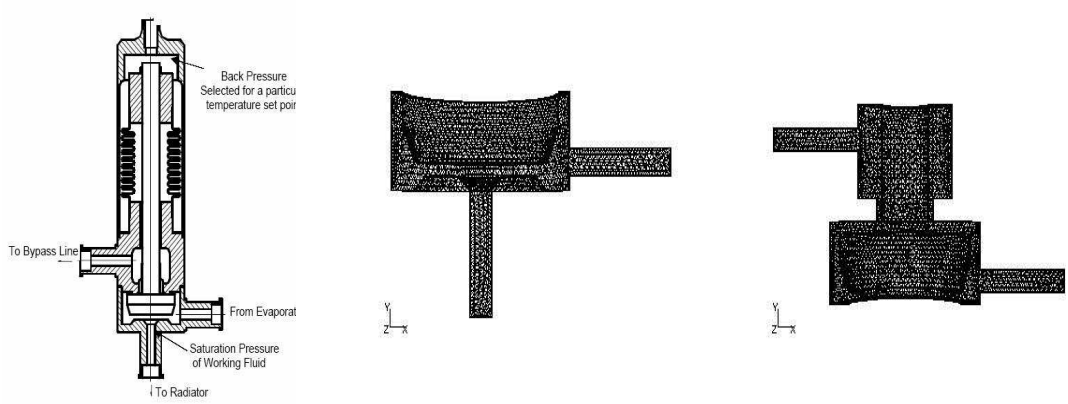

a) Bypass valve *b) Closed mode* *c) Open mode*

Figure 1: *The bypass valve and the corresponding computational meshes for the closed and open operating modes. For legibility a coarser mesh than that actually used is shown.*

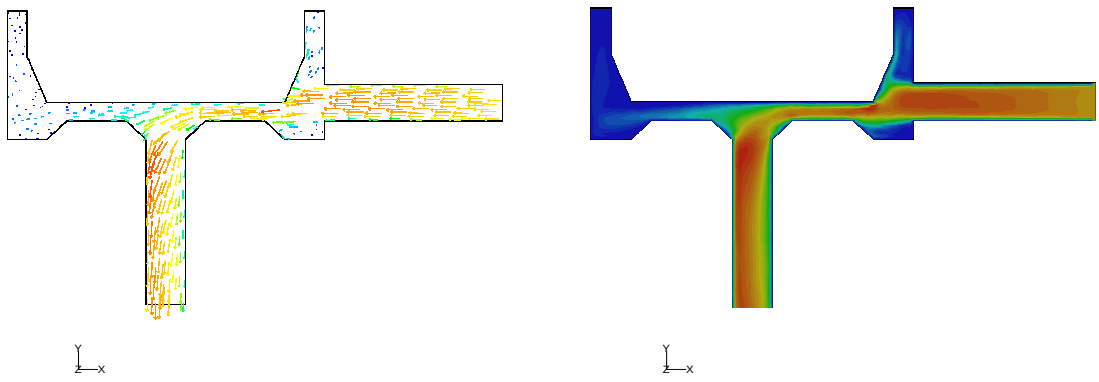

a) Velocity vectors. *b) Velocity magnitude.*

Figure 2: *Velocity field in the symmetry plane for the closed mode at* $\dot{m} = 70\mu g/s$ *and* $T = 245K$*. The velocity magnitude ranges from* $0m/s$ *(blue) to* $5m/s$ *(red).*

the stem and the corresponding shaft for reaching the outlet. This leads to a distribution of inflowing fluid around the entire stem and shaft and, by virtue of mass conservation, to a significant deceleration in flow velocity in the interior of the valve. The flow becomes directional and fluid again acquires speed upon reaching the inlet of the outlet pipe. This

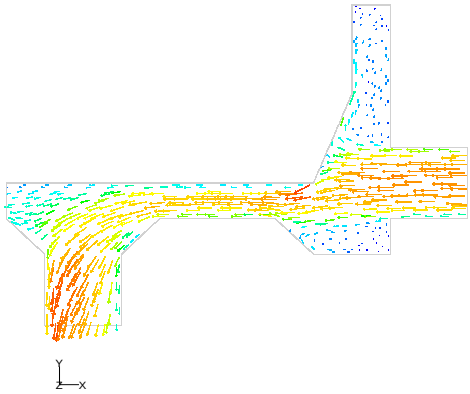

a) Velocity vectors ($T = 245\ K$).

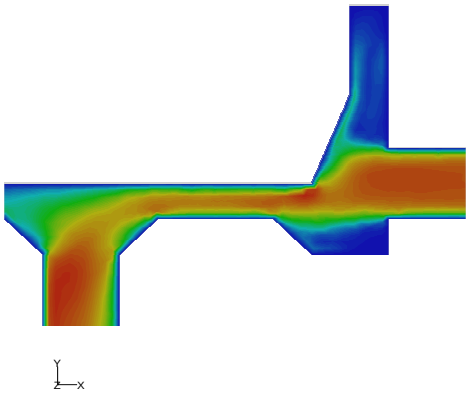

b) Velocity magnitude ($T = 265\ K$).

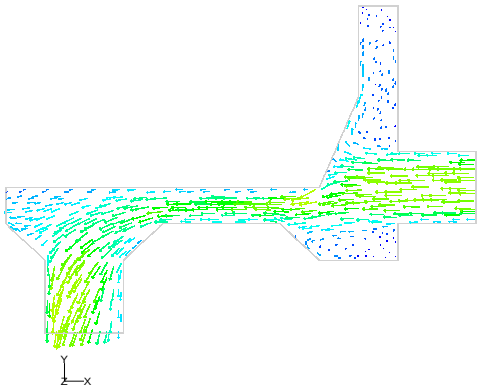

c) Velocity vectors ($T = 265\ K$).

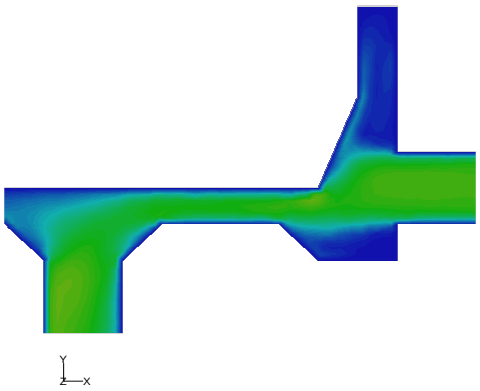

d) Velocity magnitude ($T = 265\ K$).

Figure 3: *Close-ups of the velocity field in the symmetry plane in closed mode at $\dot{m} = 70\mu g/s$ for $T = 245K$ and $T = 265K$. The velocity magnitude ranges from $0m/s$ (blue) to $5m/s$ (red).*

flow behaviour is clearly visible in shown graphs.

Close-ups of the velocity field at the inlet and outlet sections are given in Figure 6. Flow

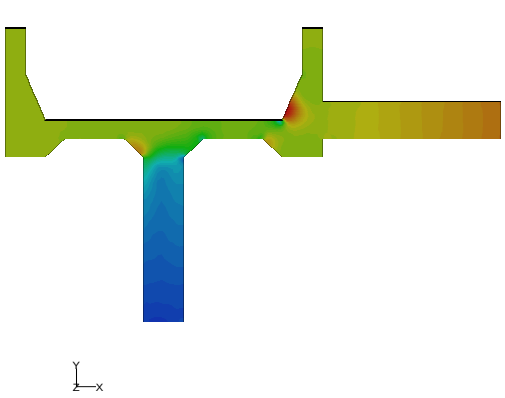

a) $T = 245K$*; full view.*

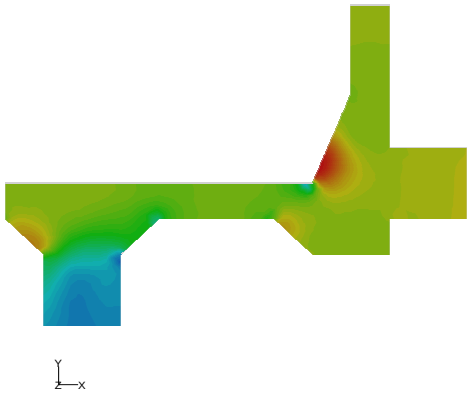

b) $T = 245K$*; close-up.*

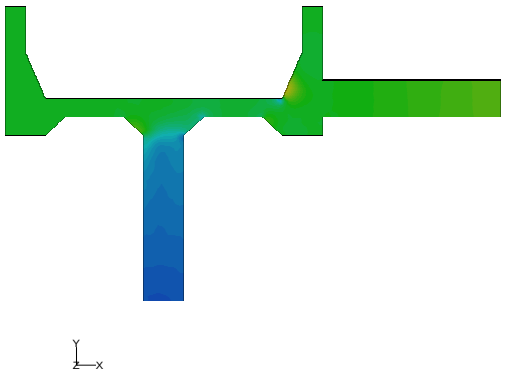

c) $T = 265K$*; symmetry plane.*

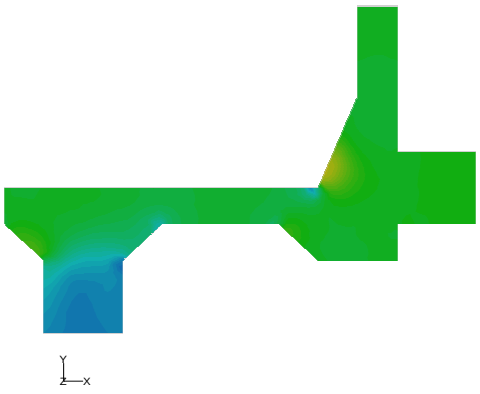

d) $T = 265K$*; close-up*

Figure 4: *Pressure field in the symmetry plane in closed mode at* $\dot{m} = 70\mu g/s$ *for* $T = 245K$ *and* $T = 265K$*. The pressure range is* $135Pa$*; blue and red indicate minimum and maximum pressure, respectively.*

properties at the inlet section are similar to the closed-mode case in that the entering flow has a developed profile that is deflected by the stem. An essential difference with the closed-mode

case is that for the present open-mode case the deflection is in both upward and downward direction. The upward deflection causes fluid to relatively directly flow along stem and shaft towards the outlet section. The downward deflection leads to the formation of a recirculation zone in the lower-right corner of the valve chamber (Figure 5*c*) via which fluid diverges in lateral-upward direction in order to flow around the stem and eventually finds its way to the outlet section as well (not shown). Fluid entering the outlet pipe is significantly accelerated and directed. This leads to a flow that rapidly becomes developed. Lowering the temperature results, similar as for the closed-mode configuration, to slightly higher fluid velocities yet with retention of the qualitative flow structure.

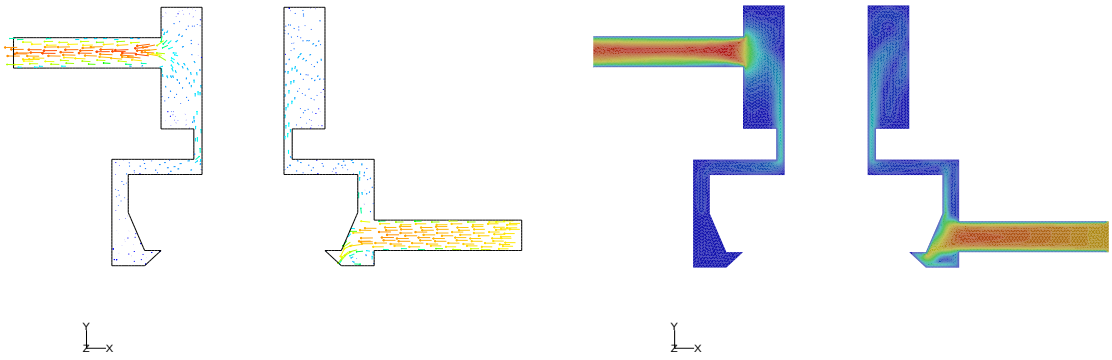

a) Velocity vectors. *b) Velocity magnitude.*

Figure 5: *Full view of the velocity field in the symmetry plane for the open mode at* $\dot{m} = 70\mu g/s$ *and* $T = 265K$*. The velocity magnitude ranges from* $0m/s$ *(blue) to* $3m/s$ *(red).*

The pressure field corresponding with the open-mode case considered above is given in Figure 7. Panel *a* gives the full view; panels *b* and *c* give close-ups of the outlet and inlet sections, respectively. Both inlet and outlet sections have approximately linear pressure drops due to the developed nature of the flow. The most important feature is the formation of a high-pressure zone at the right side of the stem, akin to that found for the closed-mode configuration, due to the sudden deflection of the flow. The pressure build-up leads, as before, to a local pressure that progressively exceeds the inlet pressure with increasing mass flow $\dot{m}$ and thus signifies a potential condensation (or freezing) zone. The risk of undesired phase changes can again be averted by ensuring slightly superheated inlet conditions. The pressure field for $T = 245$ is essentially the same yet with slightly amplified pressures.

Integral characterisation of the bypass valve

The FVM-analysis yields the following integral characterisation of the bypass valve:

- **Incompressible flow in the laminar regime.**

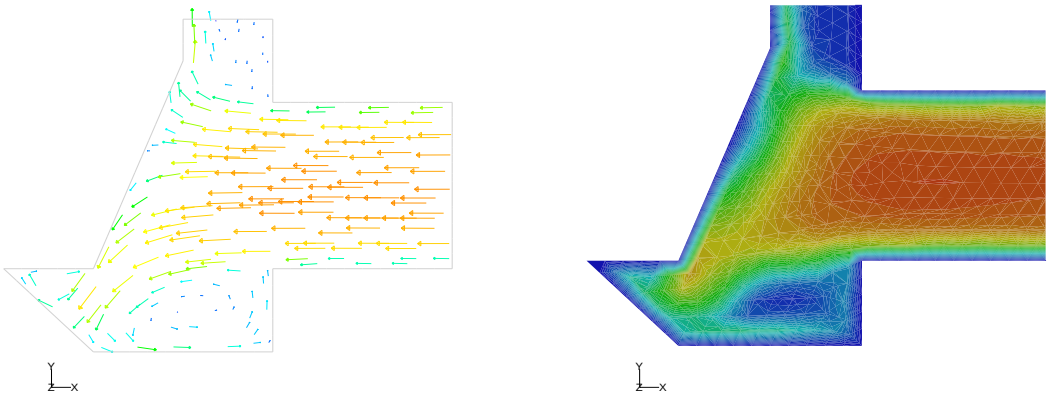

a) Velocity vectors at inlet

b) Velocity magnitude at inlet

c) Velocity vectors at outlet

d) Velocity magnitude at outlet

Figure 6: *Close up of the velocity field in the symmetry plane for the open mode at* $\dot{m} = 70\mu g/s$ *and* $T = 265K$*. The velocity magnitude ranges from* $0m/s$ *(blue) to* $3m/s$ *(red).*

- **Isothermal conditions**
- **Pressure drop between inlet and outlet** due to viscous friction. Correlation

$$\Delta p = A\,\dot{m}^2 + B, \qquad \Delta p\ [Pa], \qquad \dot{m}\ [\mu g/s], \tag{2}$$

expresses the pressure drop Δp as a function of the mass flow $\dot{m}$, with

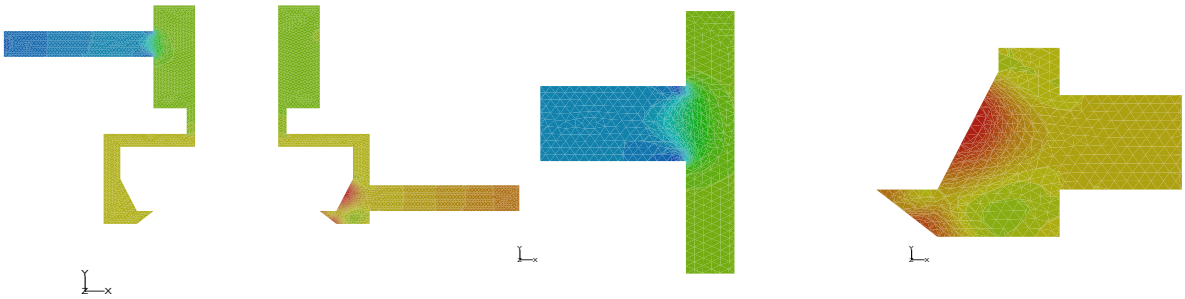

a) Pressure in full view. *b) Pressure at outlet.* *c) Pressure at inlet.*

Figure 7: *Pressure field in the symmetry plane in open mode at* $\dot{m} = 70\mu g/s$ *and* $T = 265K$*. The pressure range is* $110Pa$*; blue and red indicate minimum and maximum pressure, respectively.*

	$T = 245$; closed	$T = 245$; closed	$T = 245$; open	$T = 245$; open
A	0.016576	0.010302	0.021755	0.013172
B	16.2306	10.2695	14.6568	9.0388

the corresponding coefficients A and B for the operating conditions considered above. Correlation (2) is graphically depicted in Figure 8*a* and clearly demonstrates the quadratic increase in pressure drop with increasing mass flow. Generalisation to arbitrary inlet temperatures $245K \leq T \leq 265$ is given below.

- **Risk of condensation in case of saturation conditions at the inlet.** Remedy against this unwanted effect is ensuring a slightly superheated state at the inlet. The superheat must be higher for higher mass flows.

The changes in pressure drop appear to scale approximately linearly with changes in material properties. This follows readily from the following dimensional analysis. Steady laminar flow implies that the balance between pressure gradient and viscous forces, i.e. $\nabla p = \mu \nabla^2 \boldsymbol{u}$, predominates the fluid dynamics. Application to the above operating conditions gives

$$\Delta P \sim \frac{\mu U}{L} \quad \rightarrow \quad \frac{\Delta P_{265}}{\Delta P_{245}} = \frac{\mu_{265} U_{265}}{\mu_{245} U_{245}} \quad \overset{U=\dot{m}/A\rho}{\longrightarrow} \quad \frac{\Delta P_{265}}{\Delta P_{245}} = \frac{\mu_{265}\rho_{245}}{\mu_{245}\rho_{265}} = \frac{\nu_{265}}{\nu_{245}} = 0.64, \tag{3}$$

with $\nu = \mu/\rho$ the kinematic viscosity and ΔP the order-of-magnitude estimate of the pressure drop. Figure 8*b* reveals that the actual pressure-drop ratio $\Delta p_{265}/\Delta p_{245}$ is in good agreement with the estimate $\Delta P_{265}/\Delta P_{245} = 0.64$ throughout the operating range of the bypass valve. This suggests that within this range the pressure drop scales proportionally with the kinematic viscosity. Thus correlation (2) can to good approximation be generalised to

$$\Delta p = \frac{\mu}{\mu_{245}} \left[A_{245}\, \dot{m}^2 + B_{245} \right], \tag{4}$$

with $T = 245$ the reference state with coefficients A and B as before and μ the kinematic viscosity corresponding with the inlet temperature of interest. Correlation (4) resides between the correlations corresponding with $T = 245K$ to $T = 265K$ (Figure 4) and shifts smoothly from the $T = 245$-curve to the $T = 265$-curve with increasing T.

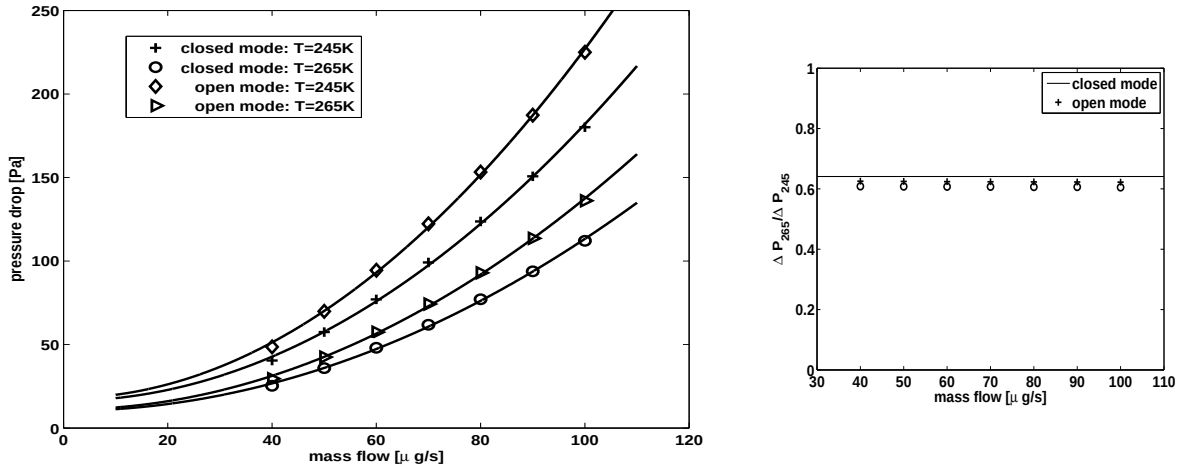

a) Closed mode. *b) Open mode.*

Figure 8: *Total pressure drop Δp between inlet and outlet as a function of the mass flow $\dot{m}$ (panel a) and ratios of pressure drop associated with minimum and maximum inlet temperatures (panel b). Symbols indicate numerical computations; curves in panel a are least-squares fits for correlation* (2)*; horizontal line in panel b indicates estimated pressure-drop ratio.*

References

ALLPROPS software-package for evaluation of thermodynamic properties, University of Idaho, College of Engineering, Center for Applied Thermodynamic Studies.

Bodendiek, F., Hollenbach, B. & Goncharov, K. 2005 Propylene loop heat pipe: technical note. Document AMS-OHB-TEN-003, OHB-System AG, Bremen.

Cengel, Y. A. & Boles, M. A. 2002 *Thermodynamics. An Engineering Approach*, McGraw Hill (fourth edition), Boston.

Kundu, P. K. 1990 *Fluid Mechanics*, Academic Press, London.

Hirsch, C. 1988 *Numerical Computation of Internal and External Flows*, Wiley, Chichester.

Schlichting, H. & Gersten, K. 2000 *Boundary-Layer Theory*, Springer, Berlin.

Speetjens M. & Rindt, C. 2006 Analytical model for the bypass valve. *INTERREG IIIC MATEO-ANTASME Deliverable 9.1.*

VDI Wärmeatlas, Ninth Edition, 2002. Springer, Berlin.